Diffusion in lattice Lorentz gases with mixtures of point scatterers

L. Acedo and A. Santos
Departamento de Física, Universidad de Extremadura, E-06071 Badajoz, Spain
(Received 10 August 1994)

Monte Carlo simulations are carried out to evaluate the diffusion coefficient in some lattice Lorentz gases with mixtures of point scatterers in the limit of a low concentration of scatterers. Two models on a square lattice are considered: (a) right and left stochastic rotators plus pure reflectors and (b) right and left stochastic mirrors plus pure reflectors. The simulation data are compared with the repeated ring approximation (RRA). The agreement is excellent for models in the absence of pure reflectors, suggesting that the RRA gives the correct diffusion coefficient for those cases. As the fraction x_B of reflectors increases, the diffusion coefficient decreases and seems to vanish at $x_B^c \simeq 0.8$ (percolation threshold) with a critical exponent $\mu \simeq 2$ (stochastic model) or $\mu \simeq 3$ (deterministic rotator model).

PACS number(s): 05.20.−y, 05.40.+j, 51.10.+y

I. INTRODUCTION

Lattice gas cellular automata have been a subject of great interest in the last few years as models of nonequilibrium fluids [1]. In the special case of Lorentz lattice gases, a moving particle follows ballistic trajectories in a d-dimensional regular lattice with a fraction ρ of the sites occupied by fixed scatterers randomly distributed. Upon hitting a scatterer, the moving particle modifies its direction of motion according to stochastic or deterministic collision rules. In addition, the scatterers can be of a single type or not, and they can have excluded volume or not [2,3].

The main transport property in Lorentz gases is the diffusion coefficient $D(\rho)$, which is defined by the Einstein relation

$$\langle r^2(t)\rangle \approx 2dD(\rho)t\ ,\quad t\to\infty\ , \tag{1}$$

where the system has been assumed isotropic. In the case of lattice Lorentz gases, the Green-Kubo formula for the diffusion coefficient reads

$$D(\rho)=\frac{1}{d}\left(\sum_{t=0}^{\infty}\Phi(t)-\frac{1}{2}\right)\ , \tag{2}$$

where

$$\Phi(t)=\langle \mathbf{v}(t)\cdot\mathbf{v}(0)\rangle \tag{3}$$

is the velocity autocorrelation function. In Eq. (3), $\langle\cdots\rangle$ denotes an average over different trajectories in a given lattice realization, followed by a subsequent average over different realizations. In Eq. (2) and thereafter, the particle is assumed to move with unit speed and the nearest neighbor distance is taken as the length unit.

If the collision rules include the possibility of backscattering, correlated collisions contribute to the diffusion coefficient as much as do uncorrelated collisions, even in the low-density limit ($\rho\to 0$) [4,5]. In that case, the Boltzmann prediction for D is incorrect. Recently, van Beijeren and Ernst [6] used an exact analytic enumeration method to derive the *exact* expression for $\lim_{\rho\to 0}\rho D(\rho)\equiv D^*$ in the case of *identical point* scatterers. Subsequently, Ossendrijver, Santos, and Ernst [2] obtained analytical expressions for D^* by resumming all the contributions associated with the so-called repeated ring collisions [7]. Since repeated ring collisions constitute only a subset of all retracing trajectories, the results obtained in Ref. [2] are in general only approximate. Nevertheless, the low-density diffusion coefficient given by the repeated ring approximation (RRA) coincides with the exact result in the special case of identical point scatterers. Consequently, in that case the effects associated with nonring collisions cancel out.

The aim of this paper is to evaluate the diffusion coefficient in mixtures of point scatterers by means of Monte Carlo computer simulations. By an adequate space and time scaling, the simulations are carried out in the limit $\rho\to 0$ directly. Two models have been considered on a square lattice: (a) right and left rotators and (b) right and left mirrors, both with and without pure reflectors. To preserve the symmetries under rotation and reflection, the fractions of left and right scatterers are equal. The simulation results are compared with the RRA. It is found that the agreement is excellent in models in the absence of reflectors. As the fraction x_B of reflectors increases, the RRA systematically underestimates the diffusion coefficient. In fact, the RRA predicts a percolation threshold $x_B^c=\frac{1}{3}$, while the simulations suggest a threshold value $x_B^c\simeq 0.8$. On the other hand, the diffusion coefficient obtained from simulation decays faster (i.e., with a larger critical exponent) as it approaches percolation than predicted by the RRA.

This paper is organized as follows. The models of mixtures of point scatterers studied in this paper are briefly described in Sec. II. The corresponding diffusion coefficients according to the Boltzmann approximation (BA) are also given. The known exact result for the case of identical point scatterers is used in Sec. III to define the average scatterer approximation (ASA). Section IV sum-

marizes the results obtained from the RRA. Some details about the simulation method are given in Sec. V. Section VI is devoted to the comparison between the simulation and the BA, the ASA, and the RRA. Finally, the conclusions are discussed in Sec. VII.

II. DESCRIPTION OF THE MODELS

Let us consider a square lattice with a fraction ρ of the sites occupied by point scatterers of different types. Let x_a be the fraction of scatterers of type a, so that $\sum_a x_a = 1$. When the particle moves along the direction i and hits a scatterer a, it has a probability W_{aij} of being deflected along the direction j. The set of 4×4 matrices W_a (or, equivalently, the set of eigenvalues $w_{a\ell}, \ell = 0,1,2,3$) define the collision rules of the model.

To fix ideas, we consider two models: the rotator model and the mirror model. Their collision rules are sketched in Fig. 1 of Ref. [2]. In the rotator model, a fraction x_R of the scatterers are right rotators, a fraction x_L are left rotators, and a fraction $x_B = 1 - x_R - x_L$ are pure reflectors. If the particle hits a right (left) rotator, it has probabilities α, β, γ, and $\delta = 1-\alpha-\beta-\gamma$ of being transmitted, reflected, deflected to the right (left), and deflected to the left (right), respectively. If it hits a pure reflector, it is reflected with probability 1. The corresponding collision matrices are

$$W_R = \begin{pmatrix} \alpha & \delta & \beta & \gamma \\ \gamma & \alpha & \delta & \beta \\ \beta & \gamma & \alpha & \delta \\ \delta & \beta & \gamma & \alpha \end{pmatrix} , \tag{4}$$

$$W_L = \begin{pmatrix} \alpha & \gamma & \beta & \delta \\ \delta & \alpha & \gamma & \beta \\ \beta & \delta & \alpha & \gamma \\ \gamma & \beta & \delta & \alpha \end{pmatrix} , \tag{5}$$

$$W_B = \begin{pmatrix} 0 & 0 & 1 & 0 \\ 0 & 0 & 0 & 1 \\ 1 & 0 & 0 & 0 \\ 0 & 1 & 0 & 0 \end{pmatrix} . \tag{6}$$

Their eigenvalues are

$$w_{R\ell} = w_{L\ell}^* = \alpha + \beta(-1)^\ell + \gamma(-i)^\ell + \delta i^\ell , \tag{7}$$

$$w_{B\ell} = (-1)^\ell . \tag{8}$$

In the deterministic case ($\gamma = 1$), this model reduces to the one introduced by Gunn and Ortuño [8]. These authors construct a mean-field theory for the transition from all trajectories being localized to some being extended.

In the mirror model, there are right mirrors, left mirrors, and pure reflectors with fractions x_R, x_L, and $x_B = 1-x_R-x_L$, respectively. Right mirrors are oriented $+45°$ with respect to a given direction and left mirrors are oriented $-45°$ with respect to that direction. When a particle hits a mirror, it has a probability α of being transmitted, a probability β of retracing its trajectory, and a probability $\gamma = 1-\alpha-\beta$ of being specularly reflected. The collision matrices of the mirrors are

$$W_R = \begin{pmatrix} \alpha & \gamma & \beta & 0 \\ \gamma & \alpha & 0 & \beta \\ \beta & 0 & \alpha & \gamma \\ 0 & \beta & \gamma & \alpha \end{pmatrix} , \tag{9}$$

$$W_L = \begin{pmatrix} \alpha & 0 & \beta & \gamma \\ 0 & \alpha & \gamma & \beta \\ \beta & \gamma & \alpha & 0 \\ \gamma & \beta & 0 & \alpha \end{pmatrix} , \tag{10}$$

with eigenvalues

$$\begin{aligned} w_{R0} = w_{L0} = 1 , \quad & w_{R1} = w_{L3} = 1-2\beta , \\ w_{R2} = w_{L2} = 1-2\gamma , \quad & w_{R3} = w_{L1} = -1+2\alpha . \end{aligned} \tag{11}$$

In the deterministic case ($\gamma = 1$) and in the absence of pure reflectors ($x_B = 0$), this model reduces to the one introduced by Ruijgrok and Cohen [9]. Notice that the deterministic mirror model in the presence of reflectors does not exhibit diffusion, since all the trajectories are trapped between two reflectors with intermediate collisions at the mirrors.

In the Boltzmann approximation, which only accounts for uncorrelated collision sequences, the low-density diffusion coefficient is [2]

$$\begin{aligned} \lim_{\rho\to 0} \rho D(\rho) &= \frac{1}{4}\left(\frac{1}{\lambda_1^0} + \frac{1}{\lambda_3^0}\right) \\ &\equiv D_0^* , \end{aligned} \tag{12}$$

where

$$\lambda_\ell^0 = 1 - \sum_a x_a w_{a\ell} . \tag{13}$$

In the above models with $x_R = x_L = \frac{1}{2}(1-x_B)$, one has

$$D_0^* = \frac{1}{2}[1-\alpha+\beta+x_B(1+\alpha-\beta)]^{-1} . \tag{14}$$

The BA fails if backscattering is present, i.e., if $x_B \neq 0$ and/or $\beta \neq 0$. In particular, if all the scatterers are pure reflectors ($x_B = 1$ or $\beta = 1$), one has $D^* = 0$, while the Boltzmann approximation yields $D_0^* = \frac{1}{4}$.

III. THE AVERAGE SCATTERER APPROXIMATION

By exactly enumerating all possible trajectories on a Cayley tree, van Beijeren and Ernst [6] were able to evaluate the low-density diffusion coefficient in the special case of identical point scatterers. For models defined on square lattices, the result is

$$\begin{aligned} \lim_{\rho\to 0} \rho D(\rho) &= \frac{1}{4}\left(\frac{1}{\lambda_1} + \frac{1}{\lambda_3}\right) \\ &\equiv D^* , \end{aligned} \tag{15}$$

where

$$\lambda_\ell = 2y\frac{1-w_\ell}{1-w_\ell+(1+w_\ell)y}\ ,\ \ell=1,3\ . \tag{16}$$

In Eq. (16), y is the real root of the cubic equation

$$\frac{(1-w_2)y}{1+w_2+(1-w_2)y}-\frac{1-w_1}{1-w_1+(1+w_1)y}$$

$$-\frac{1-w_3}{1-w_3+(1+w_3)y}=0 \tag{17}$$

that satisfies the condition $y\geq 1$.

Equations (15)–(17) can be used to define the average scatterer approximation for a mixture of scatterers [2]. In the ASA, the different types of scatterers are replaced by a single average scatterer with a collision matrix $\overline{W}$ defined as

$$\overline{W}=\sum_a x_a W_a\ , \tag{18}$$

whose eigenvalues are $\overline{w}_\ell=\sum_a x_a w_{a\ell}$ Then, Eqs. (15)–(17) are used with w_ℓ replaced by $\overline{w}_\ell$.

In the rotator and the mirror models,

$$\overline{w}_\ell=\alpha(1-x_B)+[\beta(1-x_B)+x_B](-1)^\ell$$
$$+(\gamma+\delta)(1-x_B)\frac{i^\ell+(-i)^\ell}{2}\ , \tag{19}$$

where $\delta=0$ in the mirror model and we have assumed that $x_R=x_L=\frac{1}{2}(1-x_B)$. In that case, $\lambda_1=\lambda_3$, and Eq. (17) becomes a quadratic equation. If $\overline{w}_2=-\overline{w}_1$, Eq. (17) reduces to a linear equation. That happens if $3\alpha+\beta=1$, in which case the ASA yields

$$D^*_{\rm ASA}=\frac{3}{4}\frac{\alpha(1-x_B)}{1-2\alpha(1-x_B)}\ . \tag{20}$$

As can be easily verified, if $x_B=0$ and $\beta=0$, then $y=1$ and both the BA and the ASA are exact.

IV. THE REPEATED RING APPROXIMATION

The simplest correlated collision sequences are the so-called ring collisions. They are of the form AA, AAA, . . . , where the particle experiences uncorrelated collisions between successive visits to the same scatterer A. Typical nonring correlated sequences are $ABAB$ (repeated crossings) and $ABBA$ (nested rings). By using resummation methods of kinetic theory [7], one can account for all repeated ring collisions. In the low-density limit, the diffusion coefficient obtained from the RRA is [2]

$$\lim_{\rho\to 0}\rho D(\rho)=\frac{1}{4}\left(\frac{1}{\lambda_1^{\rm RRA}}+\frac{1}{\lambda_3^{\rm RRA}}\right)$$
$$\equiv D^*_{\rm RRA}\ , \tag{21}$$

where

$$\lambda_\ell^{\rm RRA}=2y\sum_a x_a\frac{1-w_{a\ell}}{1-w_{a\ell}+(1+w_{a\ell})y}\ ,\ \ell=1,3\ , \tag{22}$$

and y is the physical root of the polynomial equation

$$\sum_a x_a\left(\frac{(1-w_{a2})y}{1+w_{a2}+(1-w_{a2})y}-\frac{1-w_{a1}}{1-w_{a1}+(1+w_{a1})y}\right.$$

$$\left.-\frac{1-w_{a3}}{1-w_{a3}+(1+w_{a3})y}\right)=0\ . \tag{23}$$

For the models considered in this paper, the above equation is cubic:

$$(1-x_B)\left(\frac{(1-w_{R2})y}{1+w_{R2}+(1-w_{R2})y}\right.$$
$$-\frac{1-w_{R1}}{1-w_{R1}+(1+w_{R1})y}$$
$$\left.-\frac{1-w_{R3}}{1-w_{R3}+(1+w_{R3})y}\right)-2x_B=0\ . \tag{24}$$

The parameter y monotonically increases with the fraction x_B of reflectors and goes to infinity as x_B approaches the threshold value $x_B^c=\frac{1}{3}$. The general behavior of y when x_B is slightly smaller than $\frac{1}{3}$ is

$$y\approx A\left(\frac{1}{3}-x_B\right)^{-1}\ , \tag{25}$$

where

$$A\equiv\frac{2}{9}\left(\frac{1+w_{R2}}{1-w_{R2}}+\frac{1-w_{R1}}{1+w_{R1}}+\frac{1-w_{R3}}{1+w_{R3}}\right)\ . \tag{26}$$

Consequently,

$$D^*_{\rm RRA}\approx\frac{3}{4}A^{-1}\left(\frac{1}{3}-x_B\right)\ , \tag{27}$$

where, as will be assumed in the sequel, we have taken $x_R=x_L$. Thus, the RRA predicts that the diffusion coefficient tends to zero (i.e., the system approaches percolation) as the fraction of reflectors tends to $\frac{1}{3}$. More generally, one can write

$$D^*\approx A(x_B^c-x_B)^\mu\ ,\ x_B\to x_B^c\ . \tag{28}$$

According to the RRA, $x_B^c=\frac{1}{3}$ and $\mu=1$. As a simple illustrative case, let us consider the rotator model with $\alpha=\beta=\gamma=\delta=\frac{1}{4}$ (i.e., the rotators become isotropic scatterers). In that case, Eq. (24) reduces to a linear equation and one simply gets

$$D^*_{\rm RRA}=\frac{9}{8}\left(\frac{1}{3}-x_B\right)\ . \tag{29}$$

Nevertheless, the behavior (27) is not universal. If the parameters of the model are such that $A=0$, the right-hand-side of Eq. (25) is replaced by the subleading term,

i.e., $y \sim (\frac{1}{3} - x_B)^{-1/2}$. This only happens in the deterministic rotator model ($\gamma = 1$) introduced by Gunn and Ortuño [8], in which case

$$D^*_{\mathrm{RRA}} = \frac{1}{2(1-x_B)}\sqrt{\frac{1-3x_B}{1+x_B}}\,, \tag{30}$$

and $\mu = \frac{1}{2}$.

If the parameters of the model are such that $A^{-1} = 0$, the model becomes trivial. This happens if $\alpha+\beta = 1$ and also in the mirror model with $\beta + \gamma = 1$. In both cases the trajectories are restricted to one-dimensional subsets and the diffusion coefficient vanishes (except if $\alpha + \beta = 1$ and $x_B = 0$, in which case $D^* = \frac{\alpha}{4\beta}$). As an illustration, let us consider the mirror model with $\alpha \ll 1$. Then,

$$D^*_{\mathrm{RRA}} \approx \frac{1-3x_B}{4x_B(1-x_B)}\alpha\,,\ x_B \neq 0\,, \tag{31}$$

$$D^*_{\mathrm{RRA}} \approx \sqrt{\frac{1-\beta}{8\beta}}\alpha^{1/2}\,,\ x_B = 0\,. \tag{32}$$

V. THE SIMULATION

Since we are interested in transport properties in the limit of a low density of scatterers, we have considered the diffusion on Cayley trees [6]. On a Cayley tree (or Bethe lattice), each scatterer is connected by branches to b neighbors ($b = 4$ in the case of a square lattice), located in one of b fixed lattice directions with respect to the first one. The intervals between scatterers have a length $\ell = 1, 2, 3, \ldots$ sampled from the distribution $P(\ell) = \rho(1-\rho)^{\ell-1}$, so that the mean free path is $\langle \ell \rangle = \rho^{-1}$. The particle moves from scatterer to scatterer along the branches of the tree. Consequently, those correlated collision sequences on a regular lattice in which the particle revisits a scatterer along a "loop" (i.e., a polygonal path with a nonzero area) are simply ignored on Cayley trees. However, "loops" have a negligible probability in the low-density limit, so that the diffusion coefficient for models on Cayley trees is identical to the one on the corresponding regular lattice [5]. Rather than performing simulations for finite ρ and then extrapolating to $\rho \to 0$, we have directly worked in the limit $\rho \to 0$. This has been done by introducing the scaled distance $\ell^* = \rho\ell$ and time $t^* = \rho t$. In the low-density limit, ℓ^* and t^* become continuous variables. The probability density for ℓ^* is the Poisson distribution $P(\ell^*) = \lim_{\rho\to 0} \frac{1}{\rho} P(\ell) = e^{-\ell^*}$ and Eq. (2) becomes

$$D^* = \lim_{t^*\to\infty} D^*(t^*)\,, \tag{33}$$

where

$$D^*(t^*) \equiv \frac{1}{d}\int_0^{t^*} d\tau \Phi(\tau)\,. \tag{34}$$

In our simulations, we have evaluated $\Phi(t^*)$ at $t^* = j\Delta t, j = 0, 1, \ldots, M$ by averaging the dot product $\mathbf{v}(0)\cdot\mathbf{v}(t^*)$ over N trajectories. Obviously, the reliability of the results is limited to times for which $|\,\Phi(t^*)\,|$ is significantly larger than $N^{-1/2}$. Then $D^*(t^*)$ is numerically evaluated by applying Simpson's rule and the diffusion coefficient D^* is obtained by extrapolating to $t^* \to \infty$. We have typically taken $\Delta t = 10^{-1}$, $M = 250$, and $N = 2 \times 10^5$.

Figure 1 shows $|\,\Phi(t^*)\,|$ for the case of isotropic scatterers, i.e., rotator model with $\alpha = \beta = \gamma = \delta = \frac{1}{4}$ and $x_B = 0$. The corresponding curve for $D^*(t^*)$ is plotted in Fig. 2. For times $t^* > 15$, $D^*(t^*)$ has reached a stationary value in excellent agreement with the exact value $D^* = \frac{3}{8}$.

As another test of the simulation, it is instructive to consider the extreme case in which all the scatterers are reflectors ($x_B = 1$ or $\beta = 1$), so that all the trajectories are trapped between two reflectors and the diffusion coefficient vanishes. Figure 3 compares $|\,\Phi(t^*)\,|$ obtained

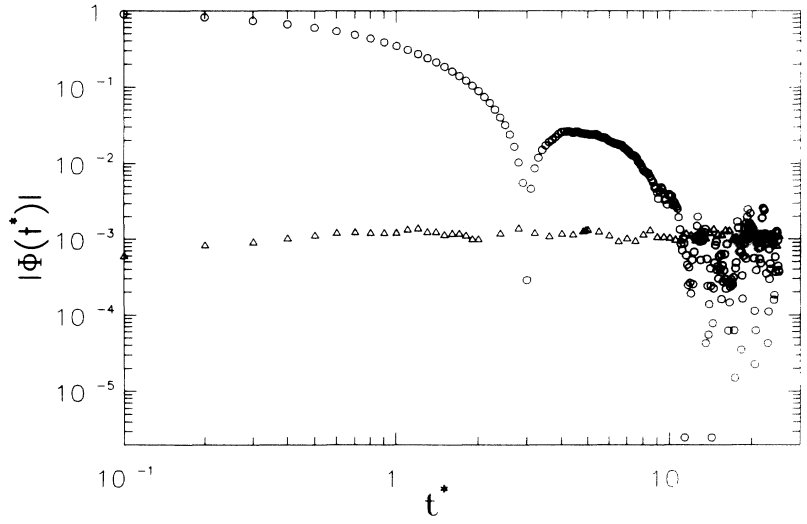

FIG. 1. Log-log plot of the absolute value of the velocity autocorrelation function $\Phi(t^*)$ for the model of isotropic scatterers. The Monte Carlo data points are denoted by open circles. The estimated errors in the Monte Carlo results are shown as open triangles.

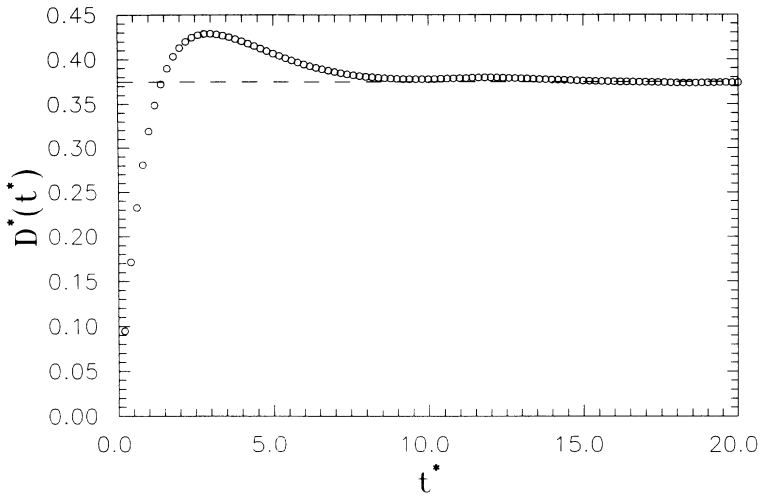

FIG. 2. Plot of the time-dependent diffusion coefficient for the model of isotropic scatterers. The Monte Carlo data points are denoted by open circles. The broken horizontal line represents the exact asymptotic value.

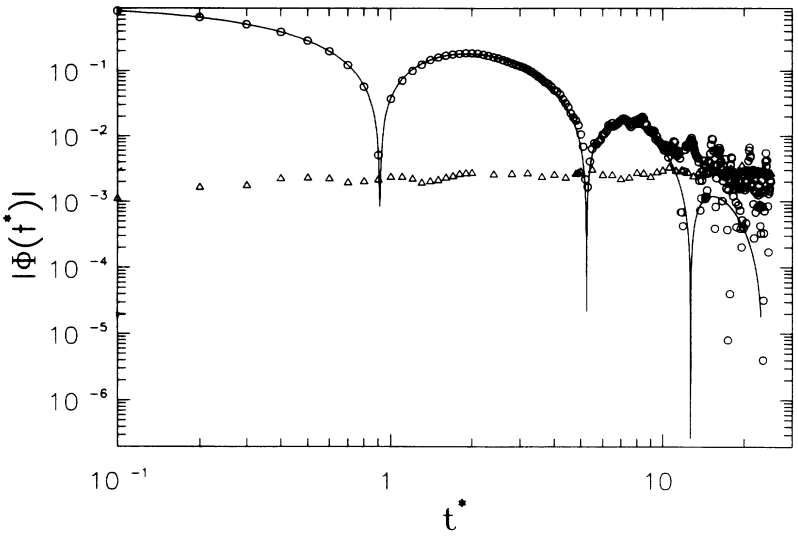

FIG. 3. Log-log plot of the absolute value of the velocity autocorrelation function $\Phi(t^*)$ for the model of pure reflectors. The solid line is the exact result. The Monte Carlo data points are denoted by open circles. The estimated errors in the Monte Carlo results are shown as open triangles.

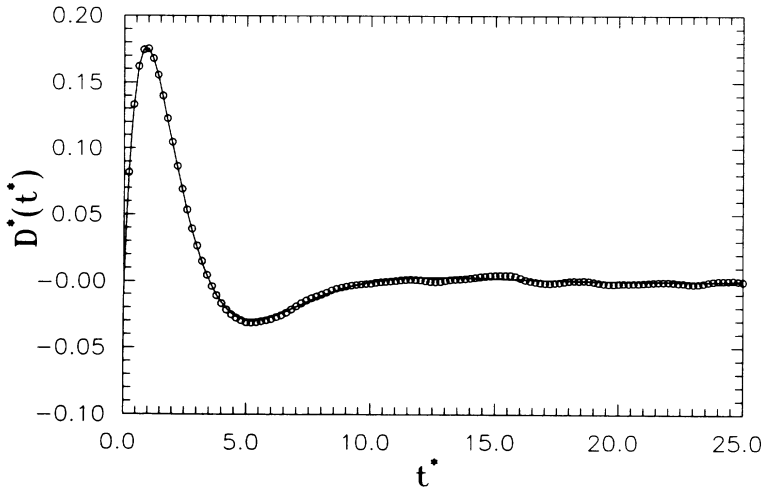

FIG. 4. Plot of the time-dependent diffusion coefficient for the model of pure reflectors. The solid line is the exact result. The Monte Carlo data points are denoted by open circles.

from simulation with the known exact result [10]. The corresponding results for $D^*(t^*)$ are shown in Fig. 4.

VI. RESULTS

A. Models without reflectors

Let us first consider models in the absence of pure reflectors ($x_B = 0$). As a consequence, the particle is never trapped in a closed trajectory. As a representative example of the rotator model we have considered the case $\alpha = \beta = (1-\gamma)/2$, $\delta = 0$. The diffusion coefficient obtained from the simulation is compared in Fig. 5 with the Boltzmann approximation, the average scatterer approximation, and the repeated ring approximation. We observe that the agreement of the RRA is excellent for all the values of γ. The ASA seems to be a fair approximation only in the region of small γ. The BA is a very poor approximation, except in the limit of deterministic rotators ($\gamma = 1$).

As a first example of the mirror model, we have chosen $\alpha = \gamma = (1-\beta)/2$. The results are plotted in Fig. 6. Again, the RRA reproduces the simulation results within the error bars. The ASA is a fair approximation that correctly takes into account that $D^* \to 0$ in the limit $\beta \to 1$.

A more interesting case is the mirror model with $\beta = \gamma = (1-\alpha)/2$. Figure 7 shows that, as before, the RRA agrees with simulation. The extrapolation of this agreement to $\alpha \to 0$ suggests that the behavior (32) might be correct. As shown in Fig. 7, the ASA predicts diffusive behavior $\left[D^*_{\mathrm{ASA}} = (1+\sqrt{33})/48 \simeq 0.14\right]$ even at $\alpha = 0$.

B. Models with reflectors

As said in Sec. IV, the RRA predicts a percolation threshold when the concentration of pure reflectors reaches the critical value $x_B^c = \frac{1}{3}$. In order to test this expectation, we have carried out simulations with different values of x_B. Let us first take the model of isotropic scatterers plus reflectors. The diffusion coefficient as a function of x_B is plotted in Fig. 8. Except when the concentration of reflectors is small, the RRA is a poor approximation. Not only is the critical value x_B^c clearly larger than $\frac{1}{3}$ but the critical exponent μ is larger than 1. On the other hand, it is interesting to note that the ASA is only correct at, but not near, $x_B = 0$ and fails to predict a percolation threshold.

Similar conclusions can be drawn from the mirror model with $\alpha = \beta = \gamma = \frac{1}{3}$, as can be seen in Fig. 9. Again, the RRA seems to reproduce the diffusion coefficient and its slope at $x_B = 0$, but underestimates D^* at finite x_B. The ASA, however, overestimates D^* even at $x_B = 0$.

As seen in Sec. IV, the RRA predicts for the *deterministic* rotator model ($\gamma = 1$) a critical exponent ($\mu = \frac{1}{2}$) different from the general one ($\mu = 1$). This is the main motivation for considering this model. Its diffusion coefficient is plotted in Fig. 10 as a function of the fraction of reflectors. As in the two previous cases, the RRA seems to be correct in the region of low concentration of pure reflectors, but strongly deviates from simulation for $x_B > 0.2$. It is interesting to note that, in contrast to what happens in the two previous cases, the ASA predicts for the deterministic rotator model a diffusion coefficient smaller than the correct one if $x_B < 0.4$.

Comparison between the simulation results of Fig. 10 and those of Figs. 8 or 9 indicates that in the first case the critical exponent μ takes a different value than in the other two cases. More specifically, μ is *larger* in the deterministic rotator model than in the stochastic rotator and mirror models. This behavior is just the opposite of what is expected from the RRA. Although our simulation data are not sufficiently close to the percolation threshold to allow for an accurate determination of μ, they are consistent with the values $\mu = 2$ for stochastic scatterers and $\mu = 3$ for the deterministic rotator model. This can be observed in Fig. 11, where $D^{*1/\mu}$ (with $\mu = 2$ or $\mu = 3$) is plotted versus x_B for the three cases considered before. It is quite interesting to note that the percolation

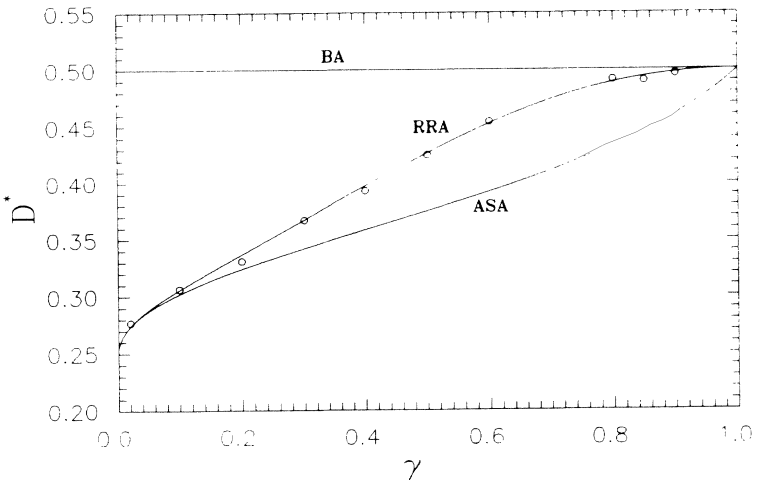

FIG. 5. Diffusion coefficient for the rotator model with $\alpha = \beta = (1-\gamma)/2$ in the absence of reflectors. The Monte Carlo data points are denoted by open circles. The solid lines correspond to the Boltzmann approximation (BA), the average scatterer approximation (ASA), and the repeated ring approximation (RRA).

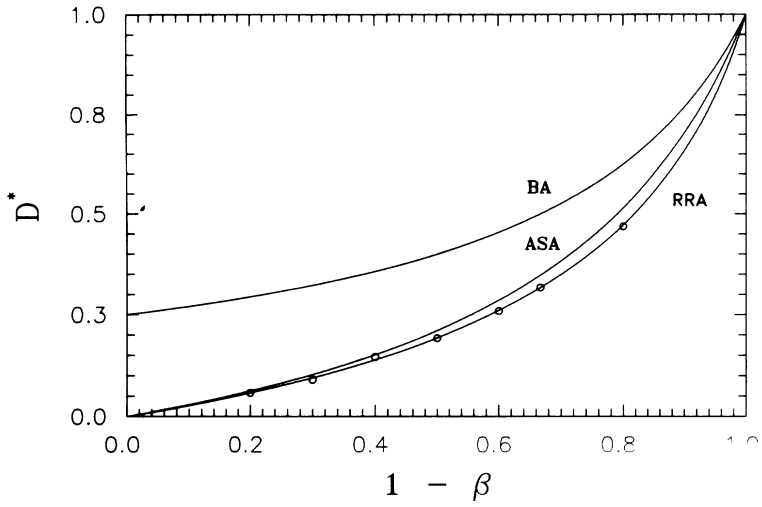

FIG. 6. Same as Fig. 5, but for the mirror model with $\alpha = \gamma = (1-\beta)/2$ in the absence of reflectors.

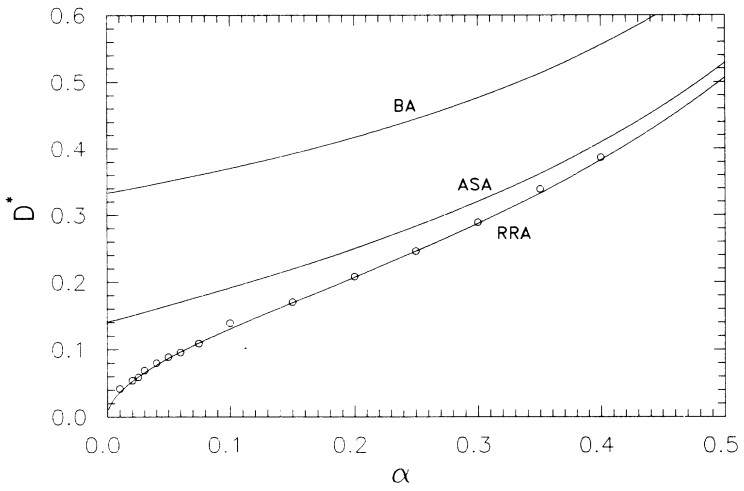

FIG. 7. Same as Fig. 5, but for the mirror model with $\beta = \gamma = (1-\alpha)/2$ in the absence of reflectors.

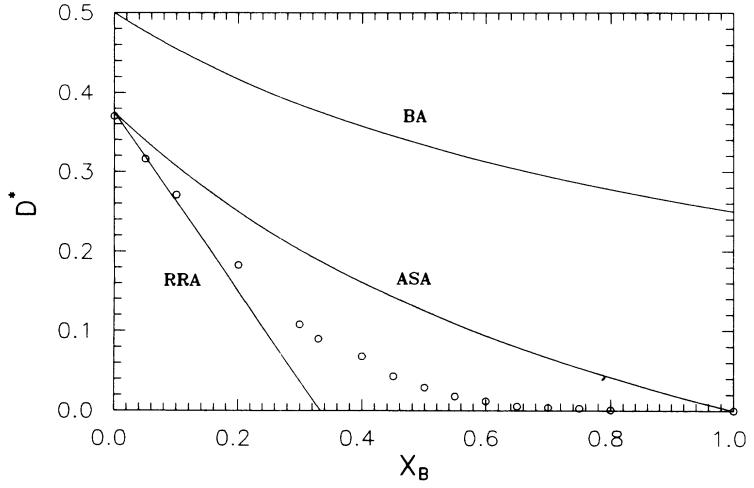

FIG. 8. Diffusion coefficient as a function of the fraction x_B of reflectors for the rotator model with $\alpha = \beta = \gamma = \delta = \frac{1}{4}$ (isotropic scatterers). The Monte Carlo data points are denoted by open circles. The solid lines correspond to the Boltzmann approximation (BA), the average scatterer approximation (ASA), and the repeated ring approximation (RRA).

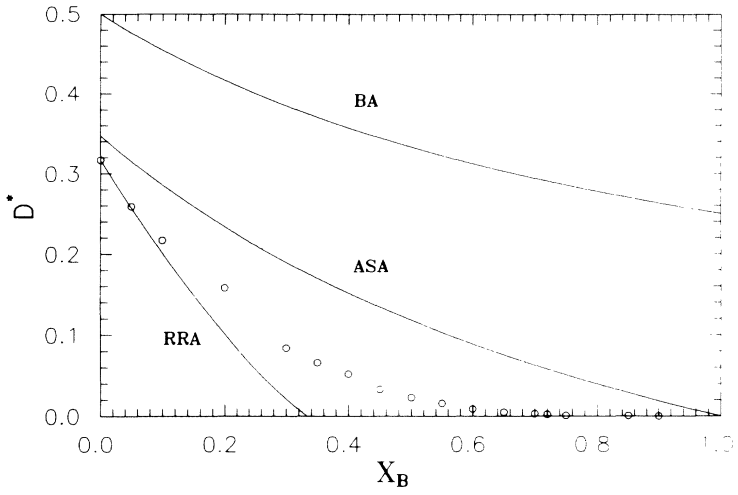

FIG. 9. Same as Fig. 8, but for the mirror model with $\alpha = \beta = \gamma = \frac{1}{3}$.

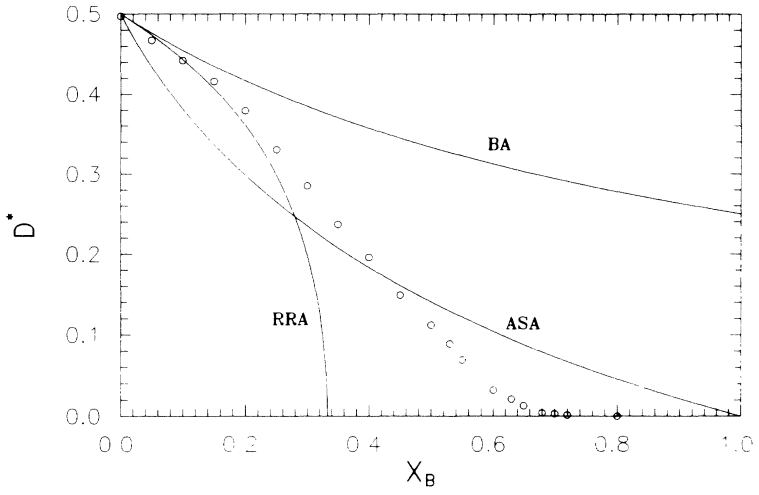

FIG. 10. Same as Fig. 8, but for the deterministic rotator model ($\gamma = 1$).

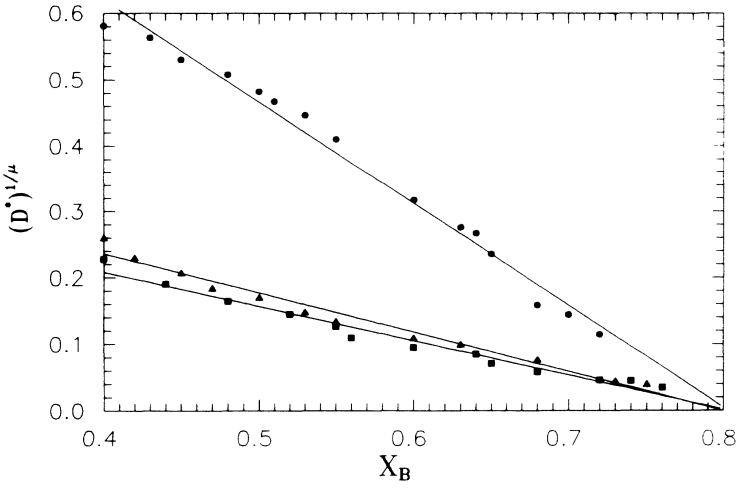

FIG. 11. Plot of $D^{*1/\mu}$ as a function of the fraction x_B of pure reflectors for isotropic scatterers ($\mu = 2$, triangles), stochastic mirrors with $\alpha = \beta = \gamma = \frac{1}{3}$ ($\mu = 2$, squares), and deterministic rotators ($\mu = 3$, circles). The Monte Carlo data points are denoted by the symbols. The solid lines are linear fits.

threshold seems to occur at the same fraction of reflectors in all cases, namely, $x_B^c \simeq 0.8$. This "universal" character of x_B^c is predicted by the RRA, although in that case the value is much smaller ($x_B^c = \frac{1}{3}$). The linear fits of the simulation data give the values $A \simeq 0.35$ (isotropic scatterers), $A \simeq 0.27$ (stochastic mirrors), and $A \simeq 3.7$ (deterministic rotators) for the amplitude defined in Eq. (28).

By using a mean-field theory for the deterministic rotator model, Gunn and Ortuño [8] have estimated that all trajectories are localized (absence of percolation) if $x_B > \frac{2}{3}$. Since diffusive behavior is a sufficient condition for percolation, our simulation results show that the percolation threshold is clearly larger than $x_B = \frac{2}{3}$.

VII. CONCLUSIONS

In this paper we have performed Monte Carlo simulations to obtain the diffusion coefficient D in some lattice Lorentz gases with mixtures of point scatterers. Two different models on square lattices have been considered: the rotator model and the mirror model, in both cases with and without pure reflectors. In all cases, the moving particle has a nonzero probability of backscattering upon collision, so that correlated collision sequences are significant even in the limit of low concentration of scatterers ($\rho \to 0$). The simulations have been carried out directly in the above limit by a convenient time and space scaling on a Cayley tree. This allows us to evaluate the scaled diffusion coefficient $D^* \equiv \lim_{\rho\to 0} \rho D(\rho)$ directly.

In the absence of backscattering, correlated collision sequences have a vanishing weight in the limit $\rho \to 0$ and the Boltzmann approximation, which accounts for all uncorrelated collisions, gives the correct diffusion coefficient. When backscattering is present, the only exact analytic enumeration of all possible trajectories we are aware of has been done by van Beijeren and Ernst [6] in the particular case of point scatterers of a *single* type. It turns out that the repeated ring approximation (RRA), which only accounts for a subclass of correlated collisions (the so-called ring collisions), yields the correct diffusion coefficient in the case of scatterers of the same type [2]. It is then natural to compare our simulation results with the RRA predictions in order to assess the degree of validity of the approximation when applied to *mixtures* of point scatterers. The following points summarize the most important conclusions drawn from our study.

(1) The agreement between the simulation data and the RRA is excellent for those models in which there are no *trapped* trajectories, i.e., models with a vanishing fraction ($x_B = 0$) of pure reflectors. This allows us to conjecture that the RRA gives the *exact* diffusion coefficient for those models, even when the scatterers are not of the same type. This would mean that the contributions to diffusion associated with all the correlated nonring collision sequences cancel out. Although we have considered only a limited number of cases, they are sufficiently representative to support our conjecture.

(2) Given a model, the diffusion coefficient is a nonlinear function $D^*(x_B)$ of the fraction of pure reflectors. Our simulations suggest that the RRA gives not only the correct diffusion coefficient at $x_B = 0$ but also the slope $(\partial D^*/\partial x_B)_{x_B=0}$.

(3) As the fraction x_B increases, the RRA systematically predicts a smaller diffusion coefficient than the correct one and becomes a poor approximation. This means that nonring collisions involving pure reflectors must have a positive net contribution to diffusion.

(4) Nevertheless, the RRA succeeds in predicting that there exists a certain threshold value x_B^c for the concentration of reflectors beyond which trapped trajectories become dominant and the diffusion coefficient vanishes. The critical exponent μ describing the behavior near threshold, see Eq. (28), takes for the deterministic rotator model a value different from the one for general stochastic models.

(5) At a quantitative level, on the other hand, the threshold behavior predicted by the RRA is clearly incorrect. According to this approximation, $x_B^c = \frac{1}{3}$, $\mu = 1$ for stochastic models, and $\mu = \frac{1}{2}$ for the deterministic rotator model. The respective values observed in the simulations are $x_B^c \simeq 0.8$, $\mu \simeq 2$, and $\mu \simeq 3$. This also shows that the percolation threshold ($x_B = \frac{2}{3}$) estimated by Gunn and Ortuño for the deterministic rotator model [8] is not correct.

ACKNOWLEDGMENTS

The authors are very grateful to Professor M. H. Ernst for a critical reading of the manuscript. Partial support from the Dirección General de Investigación Científica y Técnica (Spain) through Grant No. PB91-0316 is gratefully acknowledged. The research of L.A. has been supported by the Ministerio de Educación y Ciencia (Spain).

[1] M. H. Ernst, in *Liquids, Freezing and Glass Transition*, edited by J. P. Hansen, D. Levesque, and J. Zinn-Justin (Elsevier Science Publishers, Amsterdam, 1991), pp. 43–143.
[2] A. J. H. Ossendrijver, A. Santos, and M. H. Ernst, J. Stat. Phys. **71**, 1015 (1993).
[3] D. Frenkel, F. van Luijn, and P. M. Binder, Europhys. Lett. **20**, 7 (1992).
[4] G. A. van Velzen and M. H. Ernst, J. Phys. A **22**, 4611 (1989).
[5] M. H. Ernst, G. A. van Velzen, and P. M. Binder, Phys. Rev. A **39**, 4327 (1989).
[6] H. van Beijeren and M. H. Ernst, J. Stat. Phys. **70**, 793 (1993).
[7] G. A. van Velzen, J. Phys. A **23**, 4953 (1990).
[8] J. M. F. Gunn and M. Ortuño, J. Phys. A **18**, L1035 (1985).
[9] Th. W. Ruijgrok and E. G. D. Cohen, Phys. Lett. A **123**, 515 (1988); G. A. van Velzen, J. Phys. A **24**, 807 (1991).
[10] L. Acedo (unpublished).